1988;62:202–208.
28. Ratib O, Phelps ME, Huang SC, Henze E, Selin CE, Schelbert HR. Positron tomography with deoxyglucose for estimating local myocardial glucose metabolism. *J Nucl Med* 1982;23:577–586.
29. Yonekura Y, Tamaki N, Kambara H, et al. Detection of metabolic alterations in ischemic myocardium by F-18-fluorodeoxyglucose uptake with positron emission tomography. *Am J Cardiac Imaging* 1988;2:122–132.
30. Fudo T, Kambara H, Hashimoto T, et al. F-18-deoxyglucose and stress N-13-ammonia positron emission tomography in anterior wall healed myocardial infarction. *Am J Cardiol* 1988;61:1191–1197.
31. White CW, Wilson RF, Marcus ML. Methods of measuring myocardial blood flow in humans. *Prog Cardiovasc Dis* 1988;31:79–94.
32. Senda M, Yonekura Y, Tamaki N, et al. Interpolating and oblique-angle tomograms in myocardial PET using nitrogen-13-ammonia. *J Nucl Med* 1986;27:1830–1836.

SELF-STUDY TEST

Gastrointestinal Nuclear Medicine

Questions are taken from the *Nuclear Medicine Self-Study Program I*, published by The Society of Nuclear Medicine

DIRECTIONS

The following items consist of a heading followed by lettered options related to that heading. Select the one lettered option that is best for each item. Answers may be found on page 718.

1. **You are shown the gastric emptying time-activity curve (Fig. 1) of a 4-month-old child obtained after ingestion of 120 ml of milk containing 100 μCi of ^{99m}Tc-sulfur colloid. The child had frequent episodes of spitting up and poor weight gain. There was no history of surgery. Which *one* of the following is the best interpretation of this study?**

A. delayed gastric emptying
B. abnormally rapid gastric emptying
C. incoordinated gastric contractions
D. artifactual abnormality
E. normal study

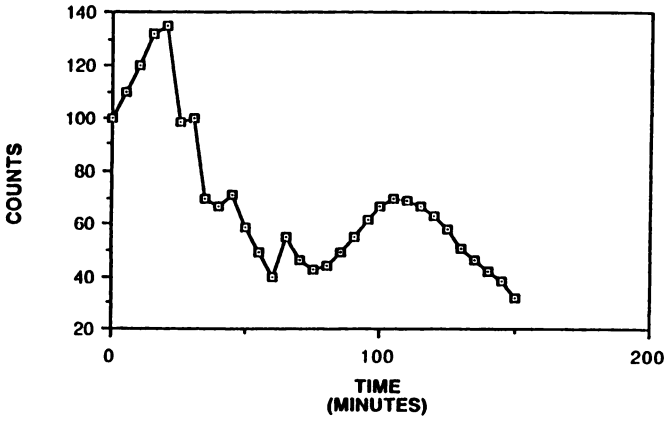

2. **A 59-year-old man with a past history of treatment for tuberculosis developed muscle wasting, diarrhea, exertional dyspnea, abdominal swelling, and edema. A chest radiograph shows a normal size heart and a gated cardiac blood-pool study demonstrates a normal ejection fraction. There is no evidence for proteinuria. Because of hypoproteinemia, a ^{51}Cr-albumin study was ordered, which shows 15% of the administered dose excreted in the feces over a 4-day period. A barium study shows only mild edema of the small intestinal mucosa. Which *one* of the following is most likely to establish the diagnosis?**

A. small bowel biopsy
B. cardiac catheterization
C. therapeutic trial of steroids
D. therapeutic trial with nonabsorbable antibiotics
E. therapeutic trial of a gluten-free diet

3. **This 1-year-old boy has right upper quadrant fullness on physical examination. An anterior static view obtained with ^{99m}Tc-sulfur colloid (Fig. 2A), an anterior view of a ^{99m}Tc-labeled red cell study (Fig. 2B), and an image from a study with ^{99m}Tc-disofenin (Fig. 2C) are shown. Which *one* of the following is the most likely diagnosis?**

A. cavernous hemangioma
B. focal nodular hyperplasia
C. congenital biliary ductal ectasia
D. metastatic neuroblastoma
E. hepatoblastoma

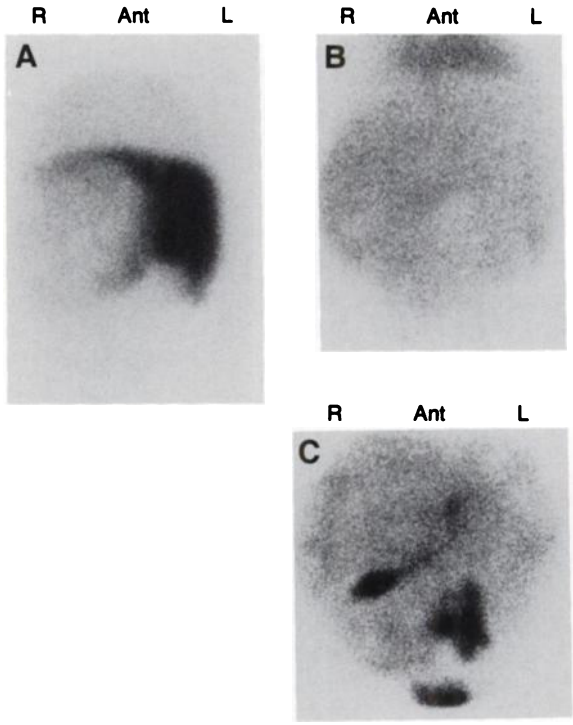

50 min

(continued on p. 718)

J Cereb Blood Flow Metab 1989;9:850–858.
17. Eckernas SA, Aquilonius SM, Hartvig P, et al. Positron emission tomography (PET) in the study of dopamine receptors in the primate brain: evaluation of a kinetic model using ^{11}C-N-methyl-spiperone. *Acta Neurol Scand* 1987;75:168–178.
18. Lidow MS, Goldman-Rakic PS, Rakic P, Innis RB. Dopamine D2 receptors in the cerebral cortex: distribution and pharmacological characterization with [^{3}H]raclopride. *Proc Natl Acad Sci USA* 1989;86:6412–6416.
19. Hartvig P, Eckernas SA, Ekblom B, et al. Receptor binding and selectivity of three ^{11}C-labeled dopamine receptor antagonists in the brain of rhesus monkeys studied with positron emission tomography. *Acta Neurol Scand* 1988;77:314–321.

SELF-STUDY TEST
Gastrointestinal Nuclear Medicine
ANSWERS

(continued from p. 685)

ITEM 1: Pediatric Gastric Emptying

ANSWER: D

The time-activity curve (Fig. 1) shows a normal initial emptying pattern of the stomach. Later, however, the stomach appears to refill. This is a common artifact due to overlapping of small bowel within the gastric region of interest. Superimposition of activity in loops of small bowel is a major problem encountered in quantitative evaluation of gastrointestinal scintigraphy. It is frequently observed in studies of enterogastric reflux, small bowel transit, and gastric emptying. Some investigators state it is not a significant problem, but anyone who has analyzed enough gastrointestinal studies recognizes it frequently. Superimposition can be recognized easily by reviewing the images and regions of interest. As Seibert et al. point out, overlap of small bowel activity with that in the stomach is a particular problem in children. Repositioning can be used to swing the stomach and duodenum away from each other.

Reference

1. Seibert JJ, Byrne WJ, Euler AR. Gastric emptying in children: unusual patterns detected by scintigraphy. *AJR* 1983;141:49–51.

ITEM 2: Protein-Losing Enteropathy

Answer: B

The ^{51}Cr-albumin study demonstrates abnormally increased fecal excretion of the radiolabeled protein. Therapy for excessive gastrointestinal protein loss depends on proper identification of the underlying disorder. Small bowel diseases, including tropical sprue, Whipple's disease, and bacterial or parasitic enteritis, are treatable with antimicrobial drugs and occasionally may show some response to steroids. A normal small bowel biopsy in this case would effectively eliminate these diseases as a cause of this patient's protein-losing enteropathy. The majority of patients with adult celiac disease (sprue) will respond to an adequate gluten-free diet. No other condition will respond so dramatically. The nonspecific findings of the barium study, however, do not indicate primary small intestinal disease in this patient. Hypoproteinemia due to protein-losing enteropathy has been described in patients with congestive heart failure, but is especially common in patients with constrictive pericarditis. Prior to the advent of antituberculous drugs, tuberculosis was the most common cause of constrictive pericarditis. The left ventricular ejection fraction may be normal because it reflects left ventricular systolic function. Heart size also may be normal. Because of the past history of tuberculosis, the most likely cause of protein-losing enteropathy in this case is constrictive pericarditis. Diastolic expansion of both ventricles is affected in constrictive pericarditis; therefore, cardiac catheterization will show elevated pressures in all four chambers. Both the right and left ventricular pressure curves will show the "square-root sign" with a rapid early diastolic dip and then a high diastolic plateau. This is the characteristic hemodynamic sign of constrictive pericarditis.

ITEM 3: Scintigraphy of Hepatoblastoma

Answer: E

The anterior ^{99m}Tc-sulfur colloid image (Fig. 2A) shows a large mass replacing the majority of the right lobe of the liver. There is increased blood-pool activity of the lesion in the right lobe compared with the uninvolved left lobe of the liver, seen in the ^{99m}Tc-red blood cell study (Fig. 2B). The activity does not approach that of the cardiac blood-pool. In addition, within the hypervascular mass are areas of reduced activity, probably indicating focal necrosis. The ^{99m}Tc-disofenin study (Fig. 2C) shows marked inhomogeneity of tracer uptake in the dominant mass. This indicates small islands of preserved hepatic parenchyma within the mass. The upper edge of the gallbladder is stretched but excretion of the tracer into the gastrointestinal tract excludes biliary obstruction.

Cavernous hemangiomas may present as solitary or multiple lesions within the liver, whereas hemangioendotheliomas are usually multifocal. Radionuclide angiography may reveal increased perfusion. If there is an enlarged blood pool, however, slow transit through such tumors may suggest a hypovascular lesion. Blood-pool imaging with labeled red blood cells confirms the vascularity of these lesions with intensity typically approaching that of the cardiac blood pool. Studies performed with hepatobiliary agents will show focal defects in the early images and these do not fill in with time because the tumors do not contain functioning hepatocytes. The blood-pool image in this case shows only slightly increased activity, making a diagnosis of cavernous hemangioma unlikely.

Focal nodular hyperplasia is rare in children. The lesions in the liver may be single or multiple, and these may exhibit either decreased, normal, or increased uptake of ^{99m}Tc-sulfur colloid. The perfusion may be normal or increased. Labeled red blood cell imaging tends to be normal, with lesion intensity equaling that of the normal hepatic parenchyma. Most lesions of focal nodular hyperplasia will show uptake of iminodiacetic acid derivatives with intensity equal to that of the surrounding liver. In some instances, however, these lesions may have relatively few hepatocytes, and a persistent defect is noted. In this case, the single defect, with slightly increased blood-pool activity and no evidence of ^{99m}Tc-disofenin accumulation, argues against focal nodular hyperplasia (as does the rarity of this disorder in children).

Congenital biliary ductal ectasia is an abnormality characterized by segmental, saccular dilatation of the intrahepatic bile ducts in the absence of obstruction. Two forms are recognized. The first (also known as Caroli's disease) is associated with bile stasis, cholangitis, intrahepatic calculus formation, and renal tubular ectasia. The second form is characterized by congenital hepatic fibrosis, cirrhosis, and portal hypertension. Images with ^{99m}Tc-sulfur colloid will show defects due to ductal enlargement and changes of cirrhosis may be present. With labeled red blood cell imaging, the lesions will not show increased vascularity. There will be delayed filling and retention of tracer in the enlarged ducts on hepatobiliary imaging. This patient clearly does not have congenital biliary ductal ectasia.

Neuroblastoma metastasizing to the liver tends to show multiple lesions by ^{99m}Tc-sulfur colloid imaging. Perfusion to the areas of involvement is decreased during the angiographic phase. Red blood cell scintigraphy reveals normal or decreased activity. Iminodiacetic acid imaging reveals focal "cold" lesions, which do not fill in with time. Although neuroblastoma cannot be definitely excluded, the single lesion in this patient with somewhat increased blood-pool activity suggests a hepatoblastoma, rather than metastatic neuroblastoma.

Hepatoblastoma usually presents as a single lesion in the liver. As with most malignant processes, the lesions appear hypovascular during the angiographic phase, although early blood flow may be seen within the tumor consistent with arterialization. Blood-pool imaging with labeled red blood cells shows a slight increase in vascularity, although the intensity is less than that of the heart. As with most malignant lesions (except some cases of differentiated hepatoma), hepatobiliary imaging with iminodiacetic acid derivatives shows a persistent defect in the liver.

Demonstration of a solitary lesion with sulfur colloid imaging is not specific. In general, added specificity can result from complementary evaluation by ultrasonography or computed tomography. The addition of further scintigraphic studies, such as labeled red blood cell and hepatocyte imaging, do add some specificity as well. The scintigraphic findings

(continued on p. 728)

because the hyperintense signal of subarachnoid space overlapped the abnormal signal density of the lesion. In contrast, ^{11}C-Met PET images showed more extensive abnormalities than MR, although angulation of the section was modestly different. Carbon-11-L-methione has the advantages of radiologic augmentation as well as paucity of tracer accumulation in normal parenchyma for detecting subtle difference of tissue density of infiltrative tumors.

From the present topographic comparison, the tracer accumulated intensely in the superficial gray matter with tumor cell infiltration as well as areas with dense aggregations of tumor cells, as was shown in Figure 3. Lower accumulation was noted in the areas where disperse tumor cells infiltrated with centrifugal growth toward the cortex. Considering that the clinical symptoms and signs deteriorated progressively during the radiotherapy the tumor, mainly consisting of cells resistant to therapy, might proliferate uniformly. Configuration of the area with high uptake of ^{11}C-Met was proportional to the extent of tumor cells aggregations. Therefore, the area of ^{11}C-Met accumulation might be highly consistent with the distribution of tumor cells even at the time of the PET study.

REFERENCES

1. Scherer HJ. The forms of growth in gliomas and their practical significance. *Brain* 1940;63:1–35.
2. Nevin S. Gliomatosis cerebri. *Brain* 1938;61:170–191.
3. Romero FJ, Ortega A, Titus F, Ibarra B, Navarro C, Rovira M. Gliomatosis cerebri with formation of a glioblastoma multiforme. Study and follow-up by magnetic resonance and computed tomography. *J Comput Tomogr* 1988;12:253–257.
4. Schmidbauer M, Muller C, Podreka I, Mamoli B, Sluga E, Deecke L. Diffuse cerebral gliomatosis presenting as motor neuron disease for two years. *J Neurol Neurosurg Psychiatry* 1989;52:275–278.
5. Spagnoli MV, Grossman RI, Packer RJ, et al. Magnetic resonance imaging determination of gliomatosis cerebri. *Neuroradiology* 1987;29:15–18.
6. Derlon JM, Bourdet C, Bustany P, et al. [^{11}C]L-methionine uptake in gliomas. *Neurosurgery* 1989;25:720–728.
7. DiChiro G, DeLaPaz RL, Brooks RA, et al. Glucose utilization of cerebral gliomas measured by [^{18}F]fluorodeoxyglucose and positron emission tomography. *Neurology* 1982;32:1323–1329.
8. Ericson K, Lilja A, Bergstrom M, et al. Positron emission tomography with ([^{11}C]methyl)-L-methionine, [^{11}C]D-glucose, and [^{68}Ga]EDTA in supratentorial tumors. *J Comput Assist Tomogr* 1985;9:683–689.
9. Mineura K, Yasuda T, Kowada M, Shishido T, Ogawa T, Uemura K. Positron emission tomographic evaluation of histological malignancy in gliomas using oxygen-15 and fluorine-18-fluorodeoxyglucose. *Neurol Res* 1986;8:164–168.
10. Mineura K, Sasajima T, Suda Y, Kowada M, Shishido F, Uemura K. Early and accurate detection of primary cerebral gliomas with interfibrillary growth using ^{11}C-L-methionine positron emission tomography. *J Med Imag* 1989;3:192–196.

SELF-STUDY TEST
Gastrointestinal Nuclear Medicine
ANSWERS

(continued from p. 718)

in this case favor the diagnosis of hepatoblastoma. Although not considered in this instance, ^{67}Ga-citrate imaging also may be useful. However, some liver tumors, for example, hepatocellular carcinoma or lymphoma, may not be distinguishable from infections.

(Images courtesy of Dr. John H. Miller, Division of Nuclear Medicine, Children's Hospital of Los Angeles.)

References

1. Miller JH, Greenspan BS. Integrated imaging of hepatic tumors in childhood. Part I: malignant lesions (primary and metastatic). *Radiology* 1985;154:83–90.
2. Miller JH, Greenspan BS. Integrated imaging of hepatic tumors in childhood. Part II: benign lesions (congenital, reparative and inflammatory). *Radiology* 1985;154:91–100.